Evolution of thermal physiology alters projected species distributions under climate change

Sara J.S. Wuitchik[1,†,*], Stephanie Mogensen[1], Tegan N. Barry[1], Antoine Paccard[2,‡], Heather A. Jamniczky[3], Rowan D.H. Barrett[2,§], and Sean M. Rogers[1,4,§]

[1]Department of Biological Sciences, University of Calgary, 2500 University Dr NW, Calgary, AB, T2N 1N4, CANADA

[2]Redpath Museum and Department of Biology, McGill University, 845 Sherbrooke St W, Montreal, QC, H3A 0G4, CANADA

[3]Department of Cell Biology & Anatomy, Cumming School of Medicine, University of Calgary, 3330 Hospital Dr NW, Calgary, T2N 4N1, CANADA

[4]Bamfield Marine Sciences Centre, 100 Pachena Rd, Bamfield, BC, V0R 1B0, CANADA

[§]equal co-senior authors

Running title: Evolution alters projected species ranges

***Corresponding author: Sara J.S. Wuitchik**

E: sjswuit@g.harvard.edu

T: 857-292-9977

†Present affiliations: Informatics Group, Harvard University, 38 Oxford St, Cambridge, MA, 02138, USA & Department of Biology, Boston University, 5 Cummington Mall, Boston, MA, 02215, USA

‡Present affiliation: McGill University Genome Center, 740 Dr Penfield Avenue, Montreal, QC, H3A 1A5, Canada

Abstract

Species distribution models (SDMs) are widely used to predict range shifts but could be unreliable under climate change scenarios because they do not account for evolution. The thermal physiology of a species is a key determinant of range and thus incorporating thermal trait evolution into SDMs might be expected to alter projected ranges. We identified a genetic basis for physiological traits that evolve in response to temperature change in threespine stickleback (*Gasterosteus aculeatus*). Using these data, we created geographic range projections under two climate change scenarios where trait data was either static ('no evolution' model), allowed to evolve at observed evolutionary rates for the trait ('evolution' model), or allowed to evolve at a rate of evolution scaled in association with the variance that is explained by quantitative trait loci (QTL; 'scaled evolution' models). We show that incorporating these traits and their evolution substantially altered the projected ranges for a widespread panmictic marine population, with over 7-fold increases in area under climate change projections. Evolution-informed SDMs should improve the precision of forecasting range dynamics under climate change, and aid in their application to management and the protection of biodiversity.

Keywords: thermal biology, critical thermal limits, evolution, species distribution models, climate change, threespine stickleback

Introduction

Temperature is a powerful driver of global biogeography and species distributions frequently reflect temperature gradients in both aquatic and terrestrial habitats (Hochachka & Somero, 2002). Many species adopt thermal strategies (such as thermoregulation or acclimation) that determine their thermal niche (Coutant, 1987; Huey & Kingsolver, 1989; Huey & Slatkin, 1976) and thermal traits can provide a target for directional selection if the environment changes to include temperatures outside the range encompassed by the thermal niche. Adaptation can thus permit species to persist at temperatures that would have previously led to extirpation (Hoffman & Sgrò, 2011; Sexton, McIntyre, Angert, & Rice, 2009). Under moderate climate change scenarios, mean global oceanic temperature is projected to increase in excess of 2°C by the end of the century (IPCC, 2014), with more extreme changes predicted in localized regions (Eyer, Blumenfeld, & Vargo, 2019; Walther et al., 2002) for both cooling and warming events (Hu, Guan, Tian, & Ren, 2018). Accurately predicting species distribution patterns under climate change therefore requires data for temperature-associated adaptive trait evolution.

While the climate and ocean temperatures are warming overall, thermal events characterized by both cold and heat extremes are occurring with increasing frequency (Hu et al., 2018; IPCC, 2014, 2018; Stott, 2016). Regionally downscaled environmental changes can be highly spatially heterogenous relative to global temperature trends, and are likely to be the most relevant for species-specific responses in the context of contemporary climate change (Walther et al., 2002). For example, range expansions of marine species have been mediated by both ocean-scale warming and also regional cooling that allowed for species invasion (Zeidberg & Robison, 2007). In such cases, population persistence will rely on both upper and lower critical thermal limits, with thermal events forcing organisms to respond independently to extreme heat and

extreme cold in separate events (Herring, Christidis, Hoell, Hoerling, & Stott, 2020; Herring et al., 2018; Herring, Hoerling, Kossing, Peterson, & Stott, 2015; Hu et al., 2018; Walther et al., 2002). Importantly, adaptation in one thermal trait can also shift the thresholds of correlated thermal traits (Buckley & Huey, 2016; Denny & Dowd, 2012; Hoffman & Sgrò, 2011; Huey & Kingsolver, 2011). Associations between traits influence the rate of trait adaptation and thus correlated traits must be considered when attempting to predict future species distributions under climate change (Hoffman & Sgrò, 2011). While there have been recent steps to incorporate theoretical trait evolution into SDMs (Bush et al., 2016; Kearney & Porter, 2009), to date, no model has used empirical estimates of evolutionary rates to inform projected species distributions under climate change scenarios.

Due to widespread phenotypic variation (Hendry, Peichel, Matthews, Boughman, & Nosil, 2013), genomic resources (Jones, Grabherr, et al., 2012), the availability of temperature-associated evolutionary trait data (Barrett et al., 2011; Morris, Bowles, Allen, Jamniczky, & Rogers, 2018), and the ability to artificially breed multiple hybrid generations in a common garden lab environment, threespine stickleback (*Gasterosteus aculeatus* Linnaeus 1758, Fig. 1a) are a useful vertebrate species for understanding the impact of adaptation on range dynamics under climate change. In particular, the availability of a regionally downscaled climate model for the Pacific Northwest (Alexander et al., 2018; IPCC, 2014; Reynolds et al., 2007) make panmictic marine populations of *G. aculeatus* in the eastern Pacific Ocean (Kirch, Romundset, Gilbert, Jones, & Foote, 2021; Morris et al., 2018) an ideal system for testing how adaptive trait variation could affect projections of species range distributions under climate change (Barrett & Hendry, 2012).

The objective of this study is to incorporate ecologically and evolutionarily relevant data on thermal traits into end-of-century projections of species distribution models. To accomplish this, we assessed physiological and behavioural temperature-associated traits in two marine and two freshwater populations of threespine stickleback, as well as within-population F1 families and marine-freshwater hybrid F1 and F2 families. We used the hybrid families to construct genetic linkage maps and identified multiple quantitative trait loci associated with thermal preference as well as upper and lower critical thermal limits. Using these genetically-based traits and empirically derived evolutionary rate data for lower critical limits in this species (Barrett et al., 2011), we constructed species distribution models that integrated the trait data reported in this study and allowed those traits to evolve under two climate change scenarios and three distinct types of evolutionary models.

Materials and Methods

Sample collection and husbandry

We collected adult *Gasterosteus aculeatus* (Fig. 1a) from two marine populations (Bamfield, M1, 48°49'12.69"N 125° 8'57.90"W; Garden Bay Lagoon, M2, 49°37'52.84"N 124° 1'49.26"W) and two freshwater populations (Hotel Lake, FW1, 49°38'26.94"N 124° 3'0.69"W; Klein Lake, FW2, 49°43'32.47"N 123°58'7.83"W) in southwestern British Columbia (Fig. 1b). Individuals were maintained in a flow-through system and photoperiod that mimicked the source populations during collection periods before transport. We transported the fish to the Life and Environmental Sciences Animal Resources Centre at the University of Calgary, where we separated the fish into population-specific 113 L glass aquaria at a density of approximately 20 fish per aquarium. We acclimated marine individuals to freshwater salinity over one week and maintained fish in a common environment (salinity of 4-6 ppt, water temperature of 15 ± 2 °C,

and a photoperiod of 16L:8D). Individuals were allowed to acclimate for at least 2 weeks before experiments (1 week for stress reduction post-transfer, 1 week for common garden environment acclimation and salinity ramp). Each common garden aquarium was on a closed system with individual filters, air stones, and water supply. We fed all adult fish *ad libitum* once per day with thawed bloodworms (Hikari Bio-Pure Frozen Bloodworms). All collections and transfers were approved by the Department of Fisheries and Oceans (marine collections and transfers), the Ministry of Forests, Lands, and Natural Resource Operations (freshwater collections), and the Huu-ay-aht First Nations (marine collections).

Crossing design for marine and freshwater F1 families

We collected eggs from females and fertilized the eggs with extracted testes from euthanized males. We transferred the fertilized egg mass to a mesh-bottomed egg incubator suspended in a 37 L aquarium for hatching. Each hatching aquarium was maintained with a single air stone and a filter. Once hatched, we reared the larval fish in 37 L hatching aquaria until they reached a total length (TL) of approximately 1 cm, after which we split the families into family-specific 113 L aquaria to maintain suitable densities. We fed the larval fish *ad libitum* twice daily with live *Artemia spp.* nauplii, and then gradually transitioned the diet to chopped, thawed bloodworms (Hikari Bio-Pure Frozen Bloodworms) *ad libitum* once daily as they reached approximately 2 cm TL. The F1 families were maintained in a common garden environment identical to that of the F0 populations. We produced one F1 family for each population (M1_F1, M2_F1, FW1_F1, and FW2_F1).

Crossing design for hybrid mapping families

To generate genetically heterogeneous marine-freshwater F1 families from wild F0 parents, we collected eggs from marine females and fertilized the eggs with extracted testes from

euthanized freshwater males. Egg masses were hatched, and juveniles were reared, as detailed above. Overall, we produced one F1 family of M1xFW1 hybrids (hereafter referred to as H1_F1) and three F1 families of M1xFW2 hybrids (hereafter referred to as H2_F1). The hybrid F1 families were maintained in a common garden environment identical to that of the F0 populations. To generate F2 families for linkage map construction, we crossed individuals from the same F1 family with the same methodology used to generate the F1 families. Overall, we produced one F2 family of H1xH1 hybrids (referred to as H1_F2) and three families of H2xH2 hybrids (referred to as H2_F2_1, H2_F2_2, and H2_F2_3). All F2 individuals were raised as described above in a common garden environment identical to that of the F0 and F1 individuals to ensure consistent history.

Thermal tolerance and preference experiments

To assess the lower and upper limits of physiological thermal tolerance, we conducted standard critical thermal minimum (CTmin) and maximum (CTmax) experiments on adult fish (Barrett et al., 2011; Fangue, Hofmeister, & Schulte, 2006; Hutchison, 1961). At these sublethal limits, the fish experiences a loss of equilibrium (LOE) at which they lose the ability to escape conditions that would ultimately lead to their death in nature (Beitinger, Bennett, & McCauley, 2000). Our experimental tank held 1000 mL glass beakers aerated individually to prevent thermal stratification. Before each experiment, individuals were fasted for 24 hours. After a 15-minute acclimation to the experimental apparatus in the individual beakers, we cooled or heated the water (for CTmin or CTmax, respectively) at a rate of approximately 0.33 °C min^{-1}. We assessed wild F0 individuals (n_{M1} = 32, n_{M2} = 14, Fig. 1c; n_{FW1} = 15, n_{FW2} = 16, N = 77; Fig. S1) and lab raised F1 (n_{M1_F1} = 13, n_{M2_F1} = 15, n_{FW1_F1} = 15, n_{FW2_F1} = 15, N = 58; Fig. S2) and F2 individuals (n_{H1_F2} = 28, $n_{H2_F2_1}$ = 36, $n_{H2_F2_2}$ = 21, $n_{H2_F2_3}$ = *17*, N = 102; Fig. S3). All

individuals were assessed for CTmin, allowed to recover for at least three days, then assessed for CTmax to keep thermal stress history consistent. The onset of erratic behaviours associated with a behavioural stress response occurred below 5.0 °C and above 25.0 °C during CTmin and CTmax experiments, respectively. Normal behaviour was observed between 5.0 °C and 25.0 °C, whereas outside of those temperatures, individuals gradually exhibited more extreme stress responses (*e.g.*, increased gilling rate, erratic movement, muscle spasms, listing, as outlined by the Canadian Council of Animal Care guidelines) until reaching LOE and the inability of an individual to right itself (the experimental endpoint) (Barrett et al., 2011; Fangue et al., 2006; Hutchison, 1961).

To assess the range of behavioural thermoregulation, we conducted thermal preference experiments in a temperature Shuttlebox (Loligo Systems, Viborg, Denmark). Experimental pools were set with a static gradient of 10 °C in the cool side and 20 °C in the warm side, connected with a water bridge at 15 °C (acclimation temperature). Temperature was continually monitored and recorded by immersed temperature probes, connected to a computer-driven temperature controller and data acquisition system (DAQ-M, Loligo Systems, Viborg, Denmark). Movement in the Shuttlebox was tracked by an infrared-sensitive uEye USB 2.0 camera (IDS Imaging Development Systems GmbH, Obersulm, Germany) which connected to Shuttlesoft (v2, Loligo Systems, Viborg, Denmark) and allowed monitoring of fish movement. Following recovery from CTmax experiments (at least three days), individuals were acclimated in the Shuttlebox for 15 minutes, with entry at ‘cool’ or ‘warm’ pool randomized, to allow for exploration of the gradient. After acclimation to the experimental apparatus, the movement of each individual was tracked in 1 second intervals for 30 minutes, recording the preferred ambient water temperature (thermal preference). Individuals were assessed individually in the Shuttlebox

apparatus to avoid any confounding social behaviours (e.g., as seen in shoaling behaviours, Cooper, Adriaenssens, & Killen, 2018). At the time of data collection for thermal trait experiments, all individuals were adults.

Relationships between all thermal traits separated by population and generation were assessed using the Pearson product-moment correlation with the *corrplot* (v0.84, Wei et al., 2017) and *Hmisc* (v3.14-0, Harrell, 2014) packages in R (R Core Team, 2019).

Isolation and characterization of single nucleotide polymorphisms (SNPs)

Genomic DNA was extracted from caudal fin tissue using a phenol-chloroform-based protocol. We digested tissues overnight in digestion buffer and proteinase K at 55 °C, then performed multiple phenol-chloroform and ethanol washes to isolate the DNA. We assessed the quantity of the extracted DNA using the Quant-iT PicoGreen dsDNA assay kit (ThermoFisher Scientific, Waltham, MA, USA) and Synergy HT plate reader with the Gen5 associated software (BioTek, Winooski, VT, USA). We prepared restriction site-associated DNA (RAD) libraries (Peterson, Weber, Kay, Fisher, & Hoekstra, 2012) using *MluCl* and *NlaIII* restriction (New England Biolabs, Ipswich, MA, USA), ligation of individual barcodes, and pooling of 48 individuals per library at equimolar concentrations. We performed a final PCR to amplify DNA and add library-specific indices to allow for pooling of multiple libraries. We sequenced three libraries at McGill University and Génome Québec Innovation Center on one lane of Illumina HiSeq 4000 (Illumina Inc., San Diego, CA, USA).

Assembly of the genetic linkage maps

After barcode demultiplexing and filtering out low quality reads in STACKS (Catchen, Hohenlohe, Bassham, Amores, & Cresko, 2013), we removed PCR duplicates from the raw sequences and aligned to the *G. aculeatus* reference genome (Jones, Grabherr, et al., 2012) using

the Burrows-Wheeler transform (Li & Durbin, 2010). Individual libraries were concatenated and filtered (Puritz, Hollenbeck, & Gold, 2014) using *vcftools* v3.0 (Danecek et al., 2011) and then split into chromosome-specific VCF files to assemble the linkage maps chromosome by chromosome. We assigned markers to a linkage group with an initial LOD score of 3 after filtering out markers that showed high levels of segregation distortion and missing observations (> 20% missing data) in Lep-MAP3 (Rastas, 2017). Unassigned markers were subsequently added to the existing linkage group at a LOD score of 3 and a size limit of 5 markers per linkage group. We ordered the markers using a minimum posterior value of 0.001 and collapsed multiple markers when the probability difference between markers was < 0.01 (Rastas, 2017). The final linkage map was phased in Lep-MAP3 (Rastas, 2017) and subset for use in R (R Core Team, 2019) with a custom Python script to generate a list of informative SNPs to use in subsequent analyses with the *qtl* v1.44-9 (Broman, Wu, Sen, & Churchill, 2003) package. The final linkage maps were similar across populations in number of markers, length, and spacing between markers, though the H2_F2 map had a higher density of markers (Table S1).

Quantitative trait loci (QTL) mapping

We analysed families separately with the same methodology to assess the presence of QTL associated with the thermal traits. We calculated conditional genotype probabilities using a hidden Markov model, allowing for possible genotyping errors at a level of 0.0001 using a Kosambi mapping function with a fixed step width, prior to running genome scans with a single QTL model (Arends, Prins, Broman, & Jansen, 2014; Broman & Sen, 2009). We determined the logarithm of the odds (LOD) score significance thresholds for each trait through permutation tests for each family (5,000 permutations per chromosome, Table 1). We pulled significant QTL above the genome-wide significance threshold ($\alpha = 0.05$, Greenwood et al., 2011), calculated

confidence intervals of QTL location based on nearby markers, and estimated the percent variance explained by each QTL peak marker. We identified two QTL associated with CTmin, two QTL associated with CTmax, three QTL associated with thermal preference, and four QTL associated with core body temperature during behavioural thermoregulation (Table 1, Fig. 2).

Environmental variables and species distribution models (SDMs)

We compiled environmental data widely used in the construction of SDMs to estimate suitable habitat in both present day and end-of-century forecasts (Wiens, Stralberg, Jongsomjit, Howell, & Snyder, 2009), including bathymetry, sea ice extent and concentration, salinity, and sea surface temperature. We used 2014 data as our baseline year to match the forecasting baseline of the Fifth Assessment Report (IPCC, 2014). We assumed a suitable habitat range for this species in the Pacific Northwest to consist of coastal areas (water depth less than 200 m) where sea ice is never present (*i.e.*, no sea ice at the maximum extent). *G. aculeatus* has a broad salinity tolerance (Bayly, 2003; Divino et al., 2016) and salinity is not limiting in any part of the range (Zweng et al., 2013), therefore salinity was not included in the final present day or forecasted models. We obtained bathymetry data from the General Bathymetric Chart of the Oceans (GEBCO) of the British Oceanographic Data Centre (Weatherall et al., 2015), and maximum sea ice extent data from the Multisensory Analyzed Sea Ice Extent – Northern Hemisphere (MASIE-NH) product (Fetterer, Savoie, Helfrich, & Clemene-Colon, 2010). We obtained maximum and minimum daily mean sea surface temperature (SST) from Reynolds et al. (2007). Sea surface temperature was used as a proxy for water temperature. Stickleback thermal trait data were used to set the limits of the distribution within the possible area delineated by sea ice free water of a suitable depth (Table S2). Thermal trait measurements were based on our experimental findings reported in the present study.

In the end-of-century forecast for suitable habitat, we assumed bathymetry to be consistent with the modern scenario. In contrast, because the Arctic Ocean is projected to be predominantly free of sea ice in the summer by the end of the century (Johannessen et al., 2004), with significant end-of-century reductions in winter/spring sea ice concentration (reduced to a concentration of 0.1 at the Seward Peninsula, Johannessen et al., 2004), we conservatively set the maximum northern extent of the suitable habitat to the western tip of the Seward Peninsula (65°35' N). The extent of sea ice was kept consistent between scenarios to control for area in calculations of range expansion. The water temperatures were increased based on projections for large marine ecosystems of Northern Oceans from global climate models (Alexander et al., 2018; IPCC, 2014). Maps were created in R (R Core Team, 2019) using the packages *raster* v. 3.3-13 (Hijmans et al., 2020) and *rgeos* v. 0.5-3 (Roger, Stuetz, Ove, Giraudoux, & Santilli, 2020).

We incorporated experimental data on the wild marine populations (Fig. 1c) to understand how inclusion of trait data may affect range projections under climate change. These trait-defined envelopes were overlain on the suitable habitat background to delineate projected presence based on thermal traits in both current day and IPCC-projected RCPs 4.5 and 8.5. The trait values were kept constant (*i.e.*, not changed) in the 'no evolution' projections. In contrast, in the 'evolution' projections, we allowed CTmin to evolve 2.5 °C lower (*i.e.*, 2.5 °C below the CTmin boundary in the 'no evolution' projection) by the end of the century, based on a rate of 0.63 *haldanes* estimated from a selection experiment previously conducted on populations belonging to the same admixed genetic cluster as the sampled populations (Barrett et al., 2011; Morris et al., 2018). Since the rate of CTmin evolution used here is an estimate based on whole-organism tolerance (Barrett et al., 2011), and thermal trait evolution is constrained by the underlying genetic architecture of the trait, we next explored how selection acting on discrete,

identifiable loci would impact evolutionary rates, and the subsequent effects on projected habitat range. To do so, we constructed models that scaled the evolutionary rate of CTmin based on the observed genetic architecture from our QTL mapping (‘scaled evolution’ projections). However, an important restriction in the evolution of CTmin for all models incorporating trait evolution (‘evolution’ and ‘scaled evolution’ projections) was a hard boundary at 0 °C, with the assumption that population persistence in a sub-zero environment would require additional adaptations to CTmin improvement (*e.g.*, extreme adaptations observed in Antarctic notothenioid fishes, Cheng & Detrich, 2007; Detrich, Parker, Williams, Nogales, & Downing, 2000; Shin et al., 2014).

To quantify the differences in estimated suitable habitat under current day and end-of-century conditions, we compared areas for each warming scenario to the equivalent scenario under current conditions. Similarly, to compare the differences in evolutionary scenarios, the area of each end-of-century evolutionary trajectory was compared to either the contrasting RCP projection or scaled evolution projection. For these comparisons, we used North Pole Lambert azimuthal equal area projection for all maps, and georeferenced to known landmarks in ArcGIS v10.8 (Environmental Systems Research Institute, 2017) to calculate area from the maps generated in R (R Core Team, 2019)(conversion ratio of 7873.42).

Results

Genetic basis of thermal traits

Stickleback exhibited a wide thermal tolerance range bounded by a mean CTmin of 1.89 °C (+/- 1.04 °C SD) and a mean CTmax of 30.1 °C (+/- 1.78 °C SD)(Fig. 1c), with these physiological traits being highly correlated (r = 0.79). These populations also tolerated a wide range of temperatures within which there was no observable stress response (5.0 – 25.0 °C).

Thermal preference values were slightly above the acclimation temperature, but with more variance around the mean than is observed in the physiological traits (16.7 +/- 3.19 °C).

To determine if these measured thermal traits have a genetic basis and could therefore evolve in response to natural selection, we raised hybrid marine-freshwater F1 (N=2) and F2 (N=4) families under common garden conditions and used these fish for genome-wide linkage map construction (Table S1) and quantitative trait loci (QTL) mapping. Using 41,840 high-quality single nucleotide variants generated from restriction site-associated DNA (RAD) sequencing, we identified two significant QTL for CTmin, two significant QTL for CTmax, and three significant QTL for thermal preference (Table 1). The trait variance that each QTL explained ranged from 28.9% (CTmin QTL on linkage group III) to 87.1% (thermal preference QTL on linkage group VII).

SDM for current day

We used these genetically based traits to first inform the boundaries of three distinct environmental regions in species distribution models (SDMs): i) a ‘normal behaviour’ envelope that included environmental temperatures associated with an absence of an observable behavioural stress response (5.0 to 25.0 °C), ii) a ‘within physiological limits’ envelope that included environmental temperatures within the range of their measured physiological limits (1.8 to 30.1°C) , and iii) an ‘outside physiological limits’ envelope with environmental temperatures that fall outside the measured physiological limits (below 1.8 and above 30.1 °C). Based on sea ice extent and bathymetry alone, our present-day suitable habitat model suggests a marine range distribution for this population from the southern Bering Sea to northern Washington state, and along the southeast Alaskan Panhandle (combined shaded area in Fig. 3a). When we include thermal trait data from the wild marine populations, nearly the entire range of suitable habitat

was unaffected by thermal tolerance limits, with the exception of a slight restriction at the northern end of the range (Fig. 3a). However, when restricted to the Normal Behaviour area, the range becomes confined to the west of the northern tip of Kodiak Island (Fig. 3a), a limit coinciding with the northern-most known marine population in the Pacific Northwest genetic cluster (Morris et al., 2018).

SDMs without trait evolution

End-of-century IPCC projections resulted in a substantial increase in the overall suitable habitat area for stickleback, with a 2.25-fold or 1,338,219 km^2 increase (combined shaded area in Fig. 3b-e) in association with a reduction in sea ice concentration at the northern end of the range. When temperature increases as projected by RCP 4.5, the 'no evolution' model projects a 5.86-fold (1,011,949 km^2) increase in the Normal Behaviour area within this newly suitable habitat (Fig. 3b) when compared to the current day model. Under RCP 8.5, the entirety of suitable habitat area remains within tolerable limits in the 'no evolution' model (Fig. 3c), with a smaller proportion of the range (10.7%) falling outside of the Normal Behaviour area as compared to RCP 4.5 conditions.

SDMs incorporating trait evolution

Incorporating the evolution of CTmin into the SDMs ('evolution' model) results in a large increase in the proportion of suitable habitat that falls within the Normal Behaviour area. We allowed CTmin to evolve by 0.63 *haldanes,* which is equal to the rate observed for CTmin in marine stickleback (Barrett et al., 2011). At this rate, the population reaches the hard limit of 0°C (1.8 °C lower than the current population CTmin) after 2-3 generations (2-3 years) - well before the end of the century. Under RCP 4.5, almost all (99.9%) of the suitable habitat range falls within the Normal Behaviour area (Fig. 3d), while under the RCP 8.5 'evolution' model, the

entire range of suitable habitat is within the Normal Behaviour area (Fig. 3e). These represent a 7.45-fold increase (1,336,123 km^2) for RCP 4.5 and 7.46-fold increase (1,338,219 km^2) for RCP 8.5 in the Normal Behaviour area when compared to the current day model.

We next scaled CTmin to evolve at a rate equivalent to the response expected if selection acted solely on the detected CTmin QTL on either linkage group III (PVE = 28.9%) or XXI (PVE = 53.7%). Under RCP 4.5 when CTmin evolved at a rate of 28.9% or 53.7% of 2.5 °C, there was a decrease in the area of the Normal Behaviour envelope of 201,230 km^2 or 123,958 km^2 (Fig. S4) in the 'scaled evolution' model when compared to the 'evolution' model. However, these decreases in the area of the Normal Behaviour envelope in comparison to the 'evolution' model still represent a substantial increase of 122,943 km^2 and 200,216 km^2 when compared to the 'no evolution' model. Allowing CTmin to evolve at these scaled rates under RCP 8.5 resulted in a decrease of 31,682 km^2 and 4,035 km^2, respectively, in the area of the Normal Behaviour envelope (Fig. S5) when compared to the 'evolution' model, which translate to an increase of 131,092 km^2 and 158,739 km^2 in comparison to the 'no evolution' model. Relative to the current day model, there was an average increase of 1,173,529 (+/- 54,640 SD) km^2 in the area of the Normal Behaviour envelope under RCP 4.5 and an average increase of 1,320,361 (+/- 19,549 SD) km^2 under RCP 8.5.

Discussion

In this study, we have produced the first 'evolution-informed' species distribution models that incorporate empirical data for temperature-associated traits and their evolution to understand how end-of-century projections change with the inclusion of this data. We assessed physiological (critical thermal minimum, CTmin, and maximum, CTmax), and behavioural (thermal preference) thermal traits for threespine stickleback from wild marine and freshwater

populations, as well as hybrid F1 and F2 families. We provide novel characterization of quantitative trait loci underlying these traits in this species, which are likely to be important genetic targets of selection under climate change. Finally, we incorporated this trait data and an empirical estimate of evolutionary rate for one of these traits into mechanistic species distribution models under two climate change scenarios (RCP 4.5 and RCP 8.5). When trait data is included in projections but held constant over warming scenarios (i.e., 'no evolution' models), there is a 6-fold (RCP 4.5) and 7-fold (RCP8.5) increase in the Normal Behaviour models. The geographic ranges projected for the end-of-century species distributions increased by over 7-fold when CTmin was allowed to evolve in the 'evolution' models. Additionally, when CTmin was allowed to evolve at a rate scaled by the percent of the trait variance that is explained by individual loci (reflective of a scenario where selection acted solely on those loci), there was a substantial increase in the area of the Normal Behaviour envelope. These changes to the projected species distributions under climate change underscore the importance of incorporating behavioural as well as physiological data into SDMs (Sunday, Bates, & Dulvy, 2012), as well as the key role that thermal trait evolution could play in range shifts (Buckley et al., 2010; Evans, Diamond, & Kelly, 2015; Lyon, Debinski, & Rangwala, 2019).

Our models project a northward range expansion under climate change. This is unsurprising because climate change opens newly available thermal niche space in waters north of the current day geographic range (Alexander et al., 2018) (as is seen in the 'no evolution' model northward expansion, Fig. 3b & d). Northward range expansion with climate change due to increasing habitat availability has also been documented in birds (Melles, Fortin, Lindsay, & Badzinski, 2011; Rushing, Andrew Royle, Ziolkowski, & Pardieck, 2020; Tingley, Monahan, Beissinger, & Moritz, 2009; Tombre, Oudman, Shimmings, Griffin, & Prop, 2019), plants

(D'Andrea et al., 2009), other fishes (Fossheim et al., 2015; Spies et al., 2020; Yapıcı, Bilge, & Filiz, 2016), and pest species (such as ticks and mountain pine beetle, Clow et al., 2017; Kurz et al., 2008; Ogden et al., 2006; Sagurova et al., 2019; Sambaraju, Carroll, & Aukema, 2019), as well as in large scale analyses of diverse taxa assessing the 'fingerprints' of climate change impacts (Parmesan & Yohe, 2003; Platts et al., 2019). What is perhaps less expected is that our models reveal that cold tolerance can have a significant impact on predicted range distributions under climate change, despite end-of-century climate change scenarios projecting an overall warmer, not cooler world. However, climate change is leading to an increase in the frequency of extreme temperature events (IPCC, 2014; Stott, 2016), including both extreme heat and extreme cold (Herring et al., 2020, 2018, 2015), which could drive selection on both CTmin and CTmax (Buckley & Huey, 2016; Denny & Dowd, 2012; Hoffman & Sgrò, 2011; Kingsolver et al., 2011). Moreover, although northern waters are warming on average, there has been considerable spatial heterogeneity in temperature change in the recent past (Walther et al., 2002). Importantly, northern waters are not predicted to be uniformly warmer under climate change (Alexander et al., 2018; IPCC, 2014) relative to the southern waters in this range, especially when seasonal variation is considered (Alexander et al., 2018). Seasonal variation and more extreme thermal events under climate change scenarios may force organisms to respond independently to both extreme heat and extreme cold in separate events (Herring et al., 2020, 2018, 2015; Walther et al., 2002), and coupled with the functional correlation between CTmin and CTmax (as observed here), population persistence will rely on adaptation in both upper and lower critical limits. Further investigations to test the empirical rate of evolution of thermal behaviour, physiology and the molecular underpinnings of these key traits would be well served by assessing additional

subpopulations along the latitudinal gradient inhabited by stickleback to gain a more detailed understanding of these temperature-associated traits over a wider environmental range.

In interpreting the projections we present here, it is important to note that we did not extend the evolutionary rate of 0.63 *haldanes* to CTmax. Without an empirical estimate of the rate of evolutionary change for CTmax in these populations or evidence for a physiologically relevant boundary (as with CTmin not evolving lower than 0 °C), extrapolating these parameters to upper thermal limits would not be accurate. Nevertheless, there is a possibility that CTmax could evolve at similar rates as CTmin, particularly in temperate marine ectotherms, given similarities in genetic architecture and the correlation between these traits in this study. However, there is a potential "hard limit" to upper thermal tolerance, as seen in tropical marine ectotherms, and CTmax evolution can also be a slow process, as seen in some terrestrial systems (Morgan, Finnøen, Jensen, Pélabon, & Jutfelt, 2021). Ultimately, given the overall warming that is projected for marine systems by the end-of-century (IPCC, 2014, 2018), there is a critical need for empirical measures of CTmax evolutionary rates for predicting future species distributions.

The efficiency of translating the selection acting on a trait into evolutionary response across generations will depend on the genetic architecture of the trait and the extent of environmental change (Rogers et al., 2012). The empirical rate of CTmin evolution in sticklebacks that we incorporated into our SDMs was estimated using change in phenotypic variation across generations (Barrett et al., 2011), rather than evolution at underlying loci. As such, it is likely that some proportion of the observed phenotypic change was due to plastic responses. In our scaled evolution models, we took a conservative approach by restricting phenotypic evolution to only occur through heritable change via the loci shown to be associated with the trait. The large effect loci that we identified here are consistent with expectations from

theory that suggest prolonged bouts of adaptation with gene flow (as expected in this system, Jones, Chan, et al., 2012; Rogers et al., 2012; Schluter, Marchinko, Barrett, & Rogers, 2010) will favour architectures characterized by fewer, larger effect, more tightly linked alleles (Via, Conte, Mason-Foley, & Mills, 2012; Yeaman & Otto, 2011; Yeaman & Whitlock, 2011). However, the effects of the QTL identified from these populations are likely overestimated, while other loci may have gone undetected (*sensu* the Beavis Effect, Beavis, 1994). Overall, the joint action of plastic effects and evolution at undetected loci might therefore result in range distributions that are more similar to those projected in our 'evolution' models.

Collectively, the inclusion of thermal traits and their evolution alters the projected ranges of marine threespine stickleback, with a substantial increase in the projected area that the species will occupy under climate change forecasts. Many traits are evolving in response to climate change (Eliason et al., 2011; Gómez-Ruiz & Lacher, 2019; Horton et al., 2020; Hovel, Carlson, & Quinn, 2016) and SDMs that do not take trait data (and trait evolution) into account could provide less accurate predictions about future species distributions under climate change (Bush et al., 2016; Guisan et al., 2013; Huey et al., 2012; Kearney & Porter, 2004) - an issue of particular concern for species at risk and pest species undergoing range expansion (Bebber, 2015; Cullingham et al., 2011; McLeod, Hallegraeff, Hosie, & Richardson, 2012). Our results provide a framework for addressing this problem, which will have critical implications for the application of these models in policy, sustainable resource management, and the protection of biodiversity in a changing climate.

References

Alexander, M. A., Scott, J. D., Friedland, K. D., Mills, K. E., Nye, J. A., Pershing, A. J., & Thomas, A. C. (2018). Projected sea surface temperatures over the 21st century: Changes in

the mean, variability and extremes for large marine ecosystem regions of Northern Oceans. *Elementa*, *6*. doi: 10.1525/elementa.191

Arends, D., Prins, P., Broman, K. W., & Jansen, R. C. (2014). Tutorial-Multiple-QTL Mapping (MQM) Analysis for R/qtl. In *http://www.rqtl.org/tutorials/MQM-tour.pdf*.

Barrett, R., & Hendry, A. (2012). Evolutionary rescue under environmental change. In *Behavioural responses to a changing world: mechanisms and consequences* (pp. 216–233). Oxford University Press Oxford, UK.

Barrett, R., Paccard, A., Healy, T., Bergek, S., Schulte, P., Schluter, D., & Rogers, S. (2011). Rapid evolution of cold tolerance in stickleback. *Proceedings of Royal Society B*, *278*(1703), 233–238. doi: 10.1098/rspb.2010.0923

Bayly, I. A. E. (2003). Salinity Tolerance and Osmotic Behavior of Animals in Athalassic Saline and Marine Hypersaline Waters. *Annual Review of Ecology and Systematics*, *3*(1), 233–268. doi: 10.1146/annurev.es.03.110172.001313

Beavis, W. (1994). The power and deceit of QTL experiments: lessons from comparative QTL studies. *49th Annual Corn & Sorghum Research Conference*, 250–266.

Bebber, D. P. (2015). Range-Expanding Pests and Pathogens in a Warming World. *Annual Review of Phytopathology*, *53*, 335–356. doi: 10.1146/annurev-phyto-080614-120207

Beitinger, T., Bennett, W., & McCauley, R. (2000). Temperature tolerances of North American freshwater fishes exposed to dynamic changes in temperature. *Environmental Biology of Fishes*, *58*, 237–275. doi: 10.1023/A:1007676325825

Broman, K. W., & Sen, S. (2009). *A Guide to QTL Mapping with R/qtl* (Vol. 46). Springer.

Broman, K. W., Wu, H., Sen, Ś., & Churchill, G. A. (2003). R/qtl: QTL mapping in experimental crosses. *Bioinformatics*, *19*(7), 889–890. doi: 10.1093/bioinformatics/btg112

Buckley, L., & Huey, R. (2016). How extreme temperatures impact organisms and the evolution of their thermal tolerance. *Integrative and Comparative Biology*, *56*(1), 98–109. doi: 10.1093/icb/icw004

Buckley, L., Urban, M., Angilletta, M., Crozier, L., Rissler, L., & MW, S. (2010). Can mechanism inform species' distribution models? *Ecology Letters*, *13*, 1041–1054. doi: 10.1111/j.1461-0248.2010.01479.x

Bush, A., Mokany, K., Catullo, R., Hoffmann, A., Kellermann, V., Sgrò, C., … Ferrier, S. (2016). Incorporating evolutionary adaptation in species distribution modelling reduces projected vulnerability to climate change. *Ecology Letters*, *19*(12), 1468–1478. doi: 10.1111/ele.12696

Catchen, J., Hohenlohe, P. A., Bassham, S., Amores, A., & Cresko, W. A. (2013). Stacks: An analysis tool set for population genomics. *Molecular Ecology*, *22*(11), 3124–3140. doi: 10.1111/mec.12354

Cheng, C. H. C., & Detrich, H. W. (2007). Molecular ecophysiology of Antarctic notothenioid fishes. *Philosophical Transactions of the Royal Society B: Biological Sciences*, *362*(1488), 2215–2232. doi: 10.1098/rstb.2006.1946

Clow, K. M., Leighton, P. A., Ogden, N. H., Lindsay, L. R., Michel, P., Pearl, D. L., & Jardine, C. M. (2017). Northward range expansion of Ixodes scapularis evident over a short timescale in Ontario, Canada. *PLoS ONE*, *12*(12), 1–15. doi: 10.1371/journal.pone.0189393

Cooper, B., Adriaenssens, B., & Killen, S. S. (2018). Individual variation in the compromise between social group membership and exposure to preferred temperatures. *Proceedings of the Royal Society B: Biological Sciences*, *285*(1880). doi: 10.1098/rspb.2018.0884

Coutant, C. C. (1987). Thermal preference: when does an asset become a liability? *Environmental Biology of Fishes*, *18*(5), 161–172. doi: 10.1007/BF00000356

Cullingham, C. I., Cooke, J. E. K., Dang, S., Davis, C. S., Cooke, B. J., & Coltman, D. W. (2011). Mountain pine beetle host-range expansion threatens the boreal forest. *Molecular Ecology*, *20*(10), 2157–2171. doi: 10.1111/j.1365-294X.2011.05086.x

D'Andrea, L., Broennimann, O., Kozlowski, G., Guisan, A., Morin, X., Keller-Senften, J., & Felber, F. (2009). Climate change, anthropogenic disturbance and the northward range expansion of Lactuca serriola (Asteraceae). *Journal of Biogeography*, *36*(8), 1573–1587. doi: 10.1111/j.1365-2699.2008.02060.x

Danecek, P., Auton, A., Abecasis, G., Albers, C. A., Banks, E., DePristo, M. A., … Group, 1000 Genomes Project Analysis. (2011). The variant call format and VCFtools. *Bioinformatics*, *27*(15), 2156–2158. doi: 10.1093/bioinformatics/btr330

Denny, M. W., & Dowd, W. W. (2012). Biophysics, environmental stochasticity, and the evolution of thermal safety margins in intertidal limpets. *Journal of Experimental Biology*, *215*(6), 934–947. doi: 10.1242/jeb.058958

Detrich, H. W., Parker, S. K., Williams, J., Nogales, E., & Downing, K. H. (2000). Cold adaptation of microtubule assembly and dynamics. Structural interpretation of primary sequence changes present in the α- and β-tubulins of antarctic fishes. *Journal of Biological Chemistry*, *275*(47), 37038–37047. doi: 10.1074/jbc.M005699200

Divino, J. N., Monette, M. Y., McCormick, S. D., Yancey, P. H., Flannery, K. G., Bell, M. A., … Schultz, E. T. (2016). Osmoregulatory physiology and rapid evolution of salinity tolerance in threespine stickleback recently introduced to fresh water. *Evolutionary Ecology Research*, *17*(2), 179–201.

Eliason, E. J., Clark, T. D., Hague, M. J., Hanson, L. M., Gallagher, Z. S., Jeffries, K. M., … Farrell, A. P. (2011). Differences in thermal tolerance among sockeye salmon populations. *Science*, *332*(6025), 109–112. doi: 10.1126/science.1199158

Environmental Systems Research Institute. (2017). *ArcGIS Desktop: Release 10.8.* Redlands, CA.

Evans, T. G., Diamond, S. E., & Kelly, M. W. (2015). Mechanistic species distribution modelling as a link between physiology and conservation. *Conservation Physiology*, *3*(1), 1–16. doi: 10.1093/conphys/cov056

Eyer, P. A., Blumenfeld, A. J., & Vargo, E. L. (2019). Sexually antagonistic selection promotes genetic divergence between males and females in an ant. *Proceedings of the National Academy of Sciences of the United States of America*, *116*(48), 24157–24163. doi: 10.1073/pnas.1906568116

Fangue, N. A., Hofmeister, M., & Schulte, P. M. (2006). Intraspecific variation in thermal tolerance and heat shock protein gene expression in common killifish, Fundulus heteroclitus. *The Journal of Experimental Biology*, *209*(15), 2859–2872. doi: 10.1242/jeb.02260

Fetterer, F., Savoie, M., Helfrich, S., & Clemene-Colon, P. (2010). U.S. National Ice Center and National Snow and Ice Data Center. *Multisensor Analyzed Sea Ice Extent - Northern Hemisphere (MASIE-NH)*. Boulder, Colorado, USA: NSIDC: National Snow and Ice Data Center. doi: https://doi.org/10.7265/N5GT5K3K.

Fossheim, M., Primicerio, R., Johannesen, E., Ingvaldsen, R. B., Aschan, M. M., & Dolgov, A. V. (2015). Recent warming leads to a rapid borealization of fish communities in the Arctic. *Nature Climate Change*, *5*(7), 673–677. doi: 10.1038/nclimate2647

Gómez-Ruiz, E. P., & Lacher, T. E. (2019). Climate change, range shifts, and the disruption of a pollinator-plant complex. *Scientific Reports*, *9*(1), 1–10. doi: 10.1038/s41598-019-53670-9

Greenwood, A. K., Jones, F. C., Chan, Y. F., Brady, S. D., Absher, D. M., Grimwood, J., … Peichel, C. L. (2011). The genetic basis of divergent pigment patterns in juvenile threespine sticklebacks. *Heredity*, *107*(2), 155–166. doi: 10.1038/hdy.2011.1

Guisan, A., Tingley, R., Baumgartner, J. B., Naujokaitis-Lewis, I., Sutcliffe, P. R., Tulloch, A. I. T., … Buckley, Y. M. (2013). Predicting species distributions for conservation decisions. *Ecology Letters*, *16*(12), 1424–1435. doi: 10.1111/ele.12189

Harrell, F. (2014). *Hmisc: Harrell Miscellaneous*. 2014.

Hendry, A. P., Peichel, C. L., Matthews, B., Boughman, J. W., & Nosil, P. (2013). Stickleback research: The now and the next. *Evolutionary Ecology Research*, *15*(2), 111–141.

Herring, S., Christidis, N., Hoell, A., Hoerling, M., & Stott, P. (2020). Explaining extreme events of 2018 from a climate perspective. *Bulletin of the American Meteorological Society*, *101*(1), 1–146. doi: 10.1175/1520-0477-95.9.s1.1

Herring, S., Christidis, N., Hoell, A., Kossin, J., Schreck, C., & Stott, P. (2018). Explaining extreme events of 2016 from a climate perspective. *Bulletin of the American Meteorological Society*, *99*(1), S1–S157. Retrieved from https://journals.ametsoc.org/view/journals/bams/99/1/bams-explainingextremeevents2016.1.xml

Herring, S., Hoerling, M., Kossing, J., Peterson, T., & Stott, P. (2015). *Explaining extreme events of 2014 from a climate perspective*. *96*(12), 1–180.

Hijmans, R. J., Etten, J. van, Sumner, M., Cheng, J., Bevan, A., Bevan, R., … Greenberg, J. A. (2020). *raster: Geographic data analysis and modelling*. Retrieved from https://cran.r-project.org/web/packages/raster/raster.pdf

Hochachka, P. W., & Somero, G. N. (2002). Mechanism and process in physiological evolution. *Biochemical Adaptation*, *480*.

Hoffman, A., & Sgrò, C. (2011). Climate change and evolutionary adaptation. *Nature*, *470*, 479–485.

Horton, K. G., La Sorte, F. A., Sheldon, D., Lin, T. Y., Winner, K., Bernstein, G., … Farnsworth, A. (2020). Phenology of nocturnal avian migration has shifted at the continental scale. *Nature Climate Change*, *10*(1), 63–68. doi: 10.1038/s41558-019-0648-9

Hovel, R. A., Carlson, S. M., & Quinn, T. P. (2016). Climate change alters the reproductive phenology and investment of a lacustrine fish, the three-spine stickleback. *Global Change Biology*, 1–13. doi: 10.1111/gcb.13531

Hu, D., Guan, Z., Tian, W., & Ren, R. (2018). Recent strengthening of the stratospheric Arctic vortex response to warming in the central North Pacific. *Nature Communications*, *9*(1). doi: 10.1038/s41467-018-04138-3

Huey, R. B., Kearney, M. R., Krockenberger, A., Holtum, J. A. M., Jess, M., & Wiliams, S. E. (2012). Predicting organismal vulnerability to climate warming: roles of behaviour, physiology and adaptation. *Philosophical Transactions of the Royal Society B: Biological Sciences*, *367*, 1665–1679. doi: 10.1098/rstb.2012.0005

Huey, R. B., & Kingsolver, J. G. (1989). Evolution of thermal sensitivity of ectotherm performance. *Trends in Ecology and Evolution*, *4*(5), 131–135.

Huey, R. B., & Kingsolver, J. G. (2011). Variation in universal temperature dependence of biological rates. *Proceedings of the National Academy of Sciences of the United States of America*, *108*(26), 10377–10378. doi: 10.1073/pnas.1107430108

Huey, R. B., & Slatkin, M. (1976). Costs and benefits of lizard thermoregulation. *Quarterly Review of Biology*, *51*(3), 363–384.

Hutchison, V. H. (1961). Comparative Biology Critical Thermal Maxima in Salamanders. *Physiological Zoology*, *34*(2), 92–125.

IPCC. (2014). Climate Change 2014: Synthesis Report. In *Fifth Assessment Report of the Intergovernmental Panel on Climate Change*. doi: 10.1016/S0022-0248(00)00575-3

IPCC. (2018). *IPCC special report on the impacts of global warming of 1.5 °C - Summary for policy makers*. (October 2018). Retrieved from http://www.ipcc.ch/report/sr15/

Johannessen, O., Bengtsson, L., Miles, M., Nagurnyi, A., Zakharov, V., Bobylev, L., … Cattle, H. (2004). Arctic climate change: observed and modelled temperature and sea-ice variability. *Tellus A: Dynamic Meteorology and Oceanography*, *56*(4), 328–341. doi: 10.3402/tellusa.v56i4.14418

Jones, F. C., Chan, Y. F., Schmutz, J., Grimwood, J., Brady, S. D., Southwick, A. M., … Kingsley, D. M. (2012). A genome-wide SNP genotyping array reveals patterns of global and repeated species-pair divergence in sticklebacks. *Current Biology*, *22*(1), 83–90. doi: 10.1016/j.cub.2011.11.045

Jones, F. C., Grabherr, M. G., Chan, Y. F., Russell, P., Mauceli, E., Johnson, J., … Kingsley, D. M. (2012). The genomic basis of adaptive evolution in threespine sticklebacks. *Nature*, *484*(7392), 55–61. doi: 10.1038/nature10944

Kearney, M., & Porter, W. (2009). Mechanistic niche modelling: Combining physiological and spatial data to predict species' ranges. *Ecology Letters*, *12*(4), 334–350. doi: 10.1111/j.1461-0248.2008.01277.x

Kearney, M., & Porter, W. P. (2004). Mapping the fundamental niche: Physiology, climate, and the distribution of a nocturnal lizard. *Ecology*, *85*(11), 3119–3131. doi: 10.1890/03-0820

Kingsolver, J. G., Arthur Woods, H., Buckley, L. B., Potter, K. A., MacLean, H. J., & Higgins, J. K. (2011). Complex life cycles and the responses of insects to climate change. *Integrative and Comparative Biology*, *51*(5), 719–732. doi: 10.1093/icb/icr015

Kirch, M., Romundset, A., Gilbert, M. T. P., Jones, F. C., & Foote, A. D. (2021). Ancient and modern stickleback genomes reveal the demographic constraints on adaptation. *Current Biology*, *31*(9), 2027-2036.e8. doi: 10.1016/j.cub.2021.02.027

Kurz, W. A., Dymond, C. C., Stinson, G., Rampley, G. J., Neilson, E. T., Carroll, A. L., … Safranyik, L. (2008). Mountain pine beetle and forest carbon feedback to climate change. *Nature*, *452*(7190), 987–990. doi: 10.1038/nature06777

Li, H., & Durbin, R. (2010). Fast and accurate long-read alignment with Burrows-Wheeler transform. *Bioinformatics*, *26*(5), 589–595. doi: 10.1093/bioinformatics/btp698

Lyon, N. J., Debinski, D. M., & Rangwala, I. (2019). Evaluating the Utility of Species Distribution Models in Informing Climate Change-Resilient Grassland Restoration Strategy. *Frontiers in Ecology and Evolution*, *7*(February), 1–8. doi: 10.3389/fevo.2019.00033

McLeod, D. J., Hallegraeff, G. M., Hosie, G. W., & Richardson, A. J. (2012). Climate-driven range expansion of the red-tide dinoflagellate Noctiluca scintillans into the Southern Ocean. *Journal of Plankton Research*, *34*(4), 332–337. doi: 10.1093/plankt/fbr112

Melles, S. J., Fortin, M. J., Lindsay, K., & Badzinski, D. (2011). Expanding northward: Influence of climate change, forest connectivity, and population processes on a threatened species' range shift. *Global Change Biology*, *17*(1), 17–31. doi: 10.1111/j.1365-2486.2010.02214.x

Morgan, R., Finnøen, M. H., Jensen, H., Pélabon, C., & Jutfelt, F. (2021). Low potential for

evolutionary rescue from climate change in a tropical fish. *Proceedings of the National Academy of Sciences of the United States of America*, *117*(52), 33365–33372. doi: 10.1073/PNAS.2011419117

Morris, M. R. J., Bowles, E., Allen, B. E., Jamniczky, H. A., & Rogers, S. M. (2018). Contemporary ancestor? Adaptive divergence from standing genetic variation in Pacific marine threespine stickleback. *BMC Evolutionary Biology*, *18*(1), 1–21. doi: 10.1186/s12862-018-1228-8

Ogden, N. H., Maarouf, A., Barker, I. K., Bigras-Poulin, M., Lindsay, L. R., Morshed, M. G., … Charron, D. F. (2006). Climate change and the potential for range expansion of the Lyme disease vector Ixodes scapularis in Canada. *International Journal for Parasitology*, *36*(1), 63–70. doi: 10.1016/j.ijpara.2005.08.016

Ouellette, L. A., Reid, R. W., Blanchard, S. G., & Brouwer, C. R. (2018). LinkageMapView-rendering high-resolution linkage and QTL maps. *Bioinformatics*, *34*(2), 306–307. doi: 10.1093/bioinformatics/btx576

Parmesan, C., & Yohe, G. (2003). *A globally coherent fingerprint of climate change impacts across natural systems*. *421*, 37–42. doi: 10.1038/nature01286

Peterson, B. K., Weber, J. N., Kay, E. H., Fisher, H. S., & Hoekstra, H. E. (2012). Double digest RADseq: An inexpensive method for de novo SNP discovery and genotyping in model and non-model species. *PLoS ONE*, *7*(5). doi: 10.1371/journal.pone.0037135

Platts, P. J., Mason, S. C., Palmer, G., Hill, J. K., Oliver, T. H., Powney, G. D., … Thomas, C. D. (2019). Habitat availability explains variation in climate-driven range shifts across multiple taxonomic groups. *Scientific Reports*, *9*(1), 1–10. doi: 10.1038/s41598-019-51582-2

Puritz, J. B., Hollenbeck, C. M., & Gold, J. R. (2014). *dDocent*□: a RADseq, variant-calling pipeline designed for population genomics of non-model organisms. *PeerJ*, *2*, e431. doi: 10.7717/peerj.431

R Core Team. (2019). *R: A language and environment for statistical computing.*

Rastas, P. (2017). Lep-MAP3: Robust linkage mapping even for low-coverage whole genome sequencing data. *Bioinformatics*, *33*(23), 3726–3732. doi: 10.1093/bioinformatics/btx494

Reynolds, R., Smith, T., Liu, C., Chelton, D., Casey, K., & Schlax, M. (2007). Daily High-Resolution-Blended Analyses for Sea Surface Temperature. *Journal of Climate*, *20*(22), 5473–5496. doi: 10.1175/2007jcli1824.1

Roger, A., Stuetz, R., Ove, K., Giraudoux, P., & Santilli, S. (2020). *rgeos: Interface to geometry engine - open*.

Rogers, S. M., Tamkee, P., Summers, B., Balabahadra, S., Marks, M., Kingsley, D. M., & Schluter, D. (2012). Genetic Signature of Adaptive Peak Shift in Threespine Stickleback. *Evolution*, (Fisher 1930), 2439–2451. doi: 10.5061/dryad.6jj614kh

Rushing, C. S., Andrew Royle, J., Ziolkowski, D. J., & Pardieck, K. L. (2020). Migratory behavior and winter geography drive differential range shifts of eastern birds in response to recent climate change. *Proceedings of the National Academy of Sciences of the United States of America*, *117*(23), 12897–12903. doi: 10.1073/pnas.2000299117

Sagurova, I., Ludwig, A., Ogden, N. H., Pelcat, Y., Dueymes, G., & Gachon, P. (2019). Predicted northward expansion of the geographic range of the tick vector amblyomma americanum in North America under future climate conditions. *Environmental Health Perspectives*, *127*(10), 1–14. doi: 10.1289/EHP5668

Sambaraju, K. R., Carroll, A. L., & Aukema, B. H. (2019). Multiyear weather anomalies associated with range shifts by the mountain pine beetle preceding large epidemics. *Forest Ecology and Management*, *438*(September 2018), 86–95. doi: 10.1016/j.foreco.2019.02.011

Schluter, D., Marchinko, K., Barrett, R., & Rogers, S. (2010). Natural selection and the genetics of adaptation in threespine stickleback. *Philosophical Transactions of the Royal Society B: Biological Sciences*, *365*(1552), 2479–2486. doi: 10.1098/rstb.2010.0036

Sexton, J. P., McIntyre, P. J., Angert, A. L., & Rice, K. J. (2009). Evolution and Ecology of Species Range Limits. *Annual Review of Ecology, Evolution, and Systematics*, *40*(1), 415–436. doi: 10.1146/annurev.ecolsys.110308.120317

Shin, S. C. hu., Ahn, D. H. wa., Kim, S. J. i., Pyo, C. W. o., Lee, H., Kim, M. K., … Park, H. (2014). The genome sequence of the Antarctic bullhead notothen reveals evolutionary adaptations to a cold environment. *Genome Biology*, *15*(9), 468. doi: 10.1186/s13059-014-0468-1

Spies, I., Gruenthal, K. M., Drinan, D. P., Hollowed, A. B., Stevenson, D. E., Tarpey, C. M., & Hauser, L. (2020). Genetic evidence of a northward range expansion in the eastern Bering Sea stock of Pacific cod. *Evolutionary Applications*, *13*(2), 362–375. doi: 10.1111/eva.12874

Stott, P. (2016). How climate change affects extreme weather events. *Science*, *352*(6293), 1517–1518. doi: 10.1126/science.aaf7271

Sunday, J. M., Bates, A. E., & Dulvy, N. K. (2012). Thermal tolerance and the global redistribution of animals. *Nature Climate Change*, *2*(9), 686–690. doi: 10.1038/nclimate1539

Tingley, M. W., Monahan, W. B., Beissinger, S. R., & Moritz, C. (2009). Birds track their Grinnellian niche through a century of climate change. *Proceedings of the National Academy of Sciences of the United States of America*, *106*(SUPPL. 2), 19637–19643. doi: 10.1073/pnas.0901562106

Tombre, I. M., Oudman, T., Shimmings, P., Griffin, L., & Prop, J. (2019). Northward range expansion in spring-staging barnacle geese is a response to climate change and population growth, mediated by individual experience. *Global Change Biology*, *25*(11), 3680–3693. doi: 10.1111/gcb.14793

Via, S., Conte, G., Mason-Foley, C., & Mills, K. (2012). Localizing FST outliers on a QTL map reveals evidence for large genomic regions of reduced gene exchange during speciation-with-gene-flow. *Molecular Ecology*, *21*(22), 5546–5560. doi: 10.1111/mec.12021

Walther, G. R., Post, E., Convey, P., Menzel, A., Parmesan, C., Beebee, T. J. C., … Bairlein, F. (2002). Ecological responses to recent climate change. *Nature*, *416*(6879), 389–395. doi: 10.1038/416389a

Weatherall, P., Marks, K., Jakobsson, M., Schmitt, T., Tani, S., Arndt, J., … Wigley, R. (2015). A new digital bathymetric model of the world's oceans. *Earth and Space Science*, *2*(8), 331–345. doi: 10.1002/2015EA000107.Received

Wei, T., Simko, V., Levy, M., Xie, Y., Jin, Y., & Zemla, J. (2017). Package 'corrplot.' *Statistician*, *56*, 316–324.

Wiens, J., Stralberg, D., Jongsomjit, D., Howell, C., & Snyder, M. (2009). Niches, models, and climate change: Assessing the assumptions and uncertainties. *Proceedings of the National Academy of Sciences*, *106*(Supplement_2), 19729–19736. doi: 10.1073/pnas.0901639106

Yapıcı, S., Bilge, G., & Filiz, H. (2016). Northwards range expansion of Sparisoma cretense (Linnaeus, 1758) in the Turkish Aegean Sea. *Journal of Aquaculture Engineering and Fisheries Research*, (August), 201–207. doi: 10.3153/jaefr16022

Yeaman, S., & Otto, S. P. (2011). Establishment and maintenance of adaptive genetic divergence under migration, selection, and drift. *Evolution*, *65*(7), 2123–2129. doi: 10.1111/j.1558-5646.2011.01277.x

Yeaman, S., & Whitlock, M. C. (2011). The genetic architecture of adaptation under migration-selection balance. *Evolution*, *65*(7), 1897–1911. doi: 10.1111/j.1558-5646.2011.01269.x

Zeidberg, L. D., & Robison, B. H. (2007). Invasive range expansion by the Humboldt squid, Dosidicus gigas, in the eastern North Pacific. *Proceedings of the National Academy of Sciences*, *104*(31), 12948–12950. doi: 10.1073/pnas.0702043104

Zweng, M. M., Reagan, J. R., Antonov, J. I., Mishonov, A. V., Boyer, T. P., Garcia, H. E., … Bidlle, M. M. (2013). World Ocean Atlas 2013, Volume 2: Salinity. In *NOAA Atlas NESDIS 74* (Vol. 2). doi: 10.1182/blood-2011-06-357442

Acknowledgments

The authors acknowledge that the species collections took place on Huu-ay-aht and Sechelt First Nations traditional territories and are grateful for the opportunity to conduct their research in protected and sacred areas. We would like to thank the Bamfield Marine Sciences Centre for the resources required to conduct this research, Sam Owens for the photo in Figure 1a, Peter Peller

for creating Figure 1b, as well as Daniel Wuitchik, Sam Yeaman, Jennifer Sunday, and Patrick Nosil for feedback on the manuscript. This research was funded by Discovery Grants from the Natural Sciences and Engineering Research Council of Canada to RDHB and SMR, a Canada Research Chair to RDHB, a New Faculty Award from Alberta Innovates Technology Futures to SMR.

Author Contributions

This study was designed by SJSW, RDHB, and SMR; fish husbandry and breeding by SJSW and TNB; experimental data collection by SJSW; DNA sequencing and initial processing by AP; bioinformatic and QTL analyses by SJSW; species distribution modelling by SJSW and SM; the manuscript was written by SJSW, RDHB, and SMR, with input from authors; the study was funded by HAJ, RDHB, and SMR.

Data Accessibility

The data associated with this work is available as follows:

DNA sequences: upload pending on NCBI SRA

Experimental data associated with thermal trait data: available on Dryad (https://doi.org/10.5061/dryad.70rxwdbz6)

Annotated code and example files: available on Github (https://github.com/sjswuitchik/gasAcu_qtl_sdm)

Figures and Tables

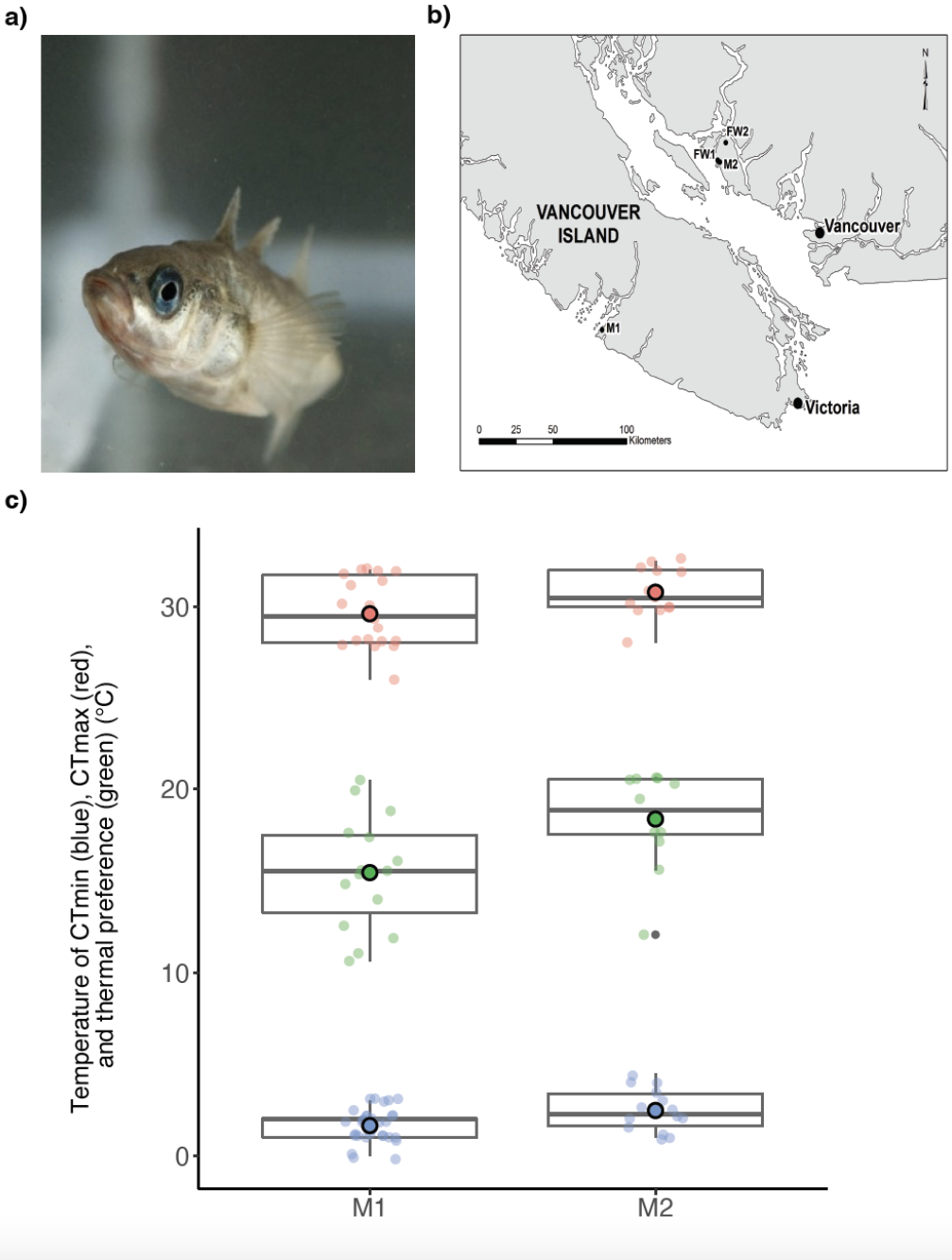

Figure 1. a) Adult threespine stickleback (*Gasterosteus aculeatus*) from a single genetic cluster were sampled from b) two marine and two freshwater populations in the Canadian Pacific Northwest. These populations were assayed for c) thermal preference (green), critical thermal minima (blue) and maxima (red). Thermal trait values for marine populations (M1 and M2) were incorporated into the species distribution models, while marine and freshwater populations (M1, FW1, and FW2) were used to generate F1 and F2 generations for linkage map construction and quantitative trait loci (QTL) analyses.

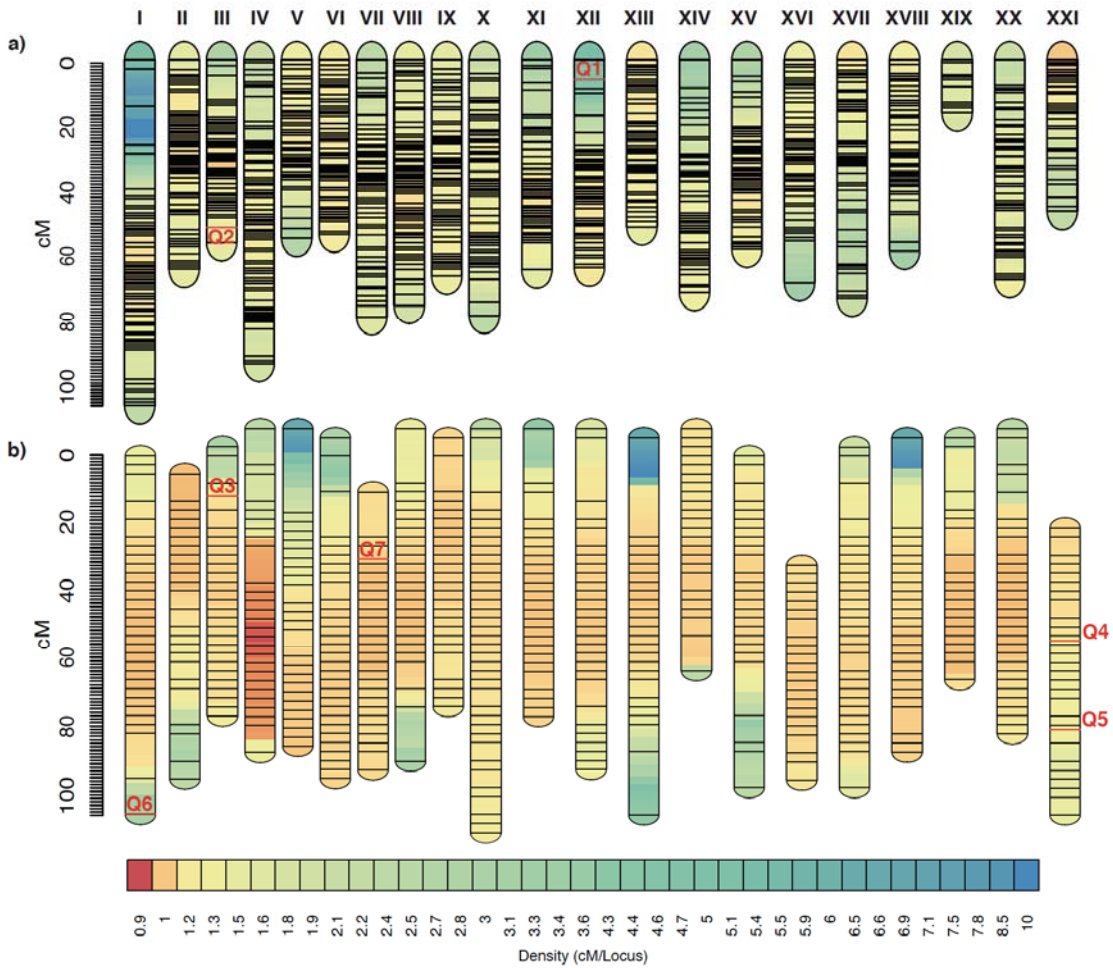

Figure 2. Linkage maps constructed for quantitative trait loci (QTL) analyses for a) H1 F2 hybrids (M1 x FW1) and b) H2 F2 hybrids (M1 x FW2) families, rendered with LinkageMapView (Ouellette, Reid, Blanchard, & Brouwer, 2018), with locations of QTL indicated (Table 1).

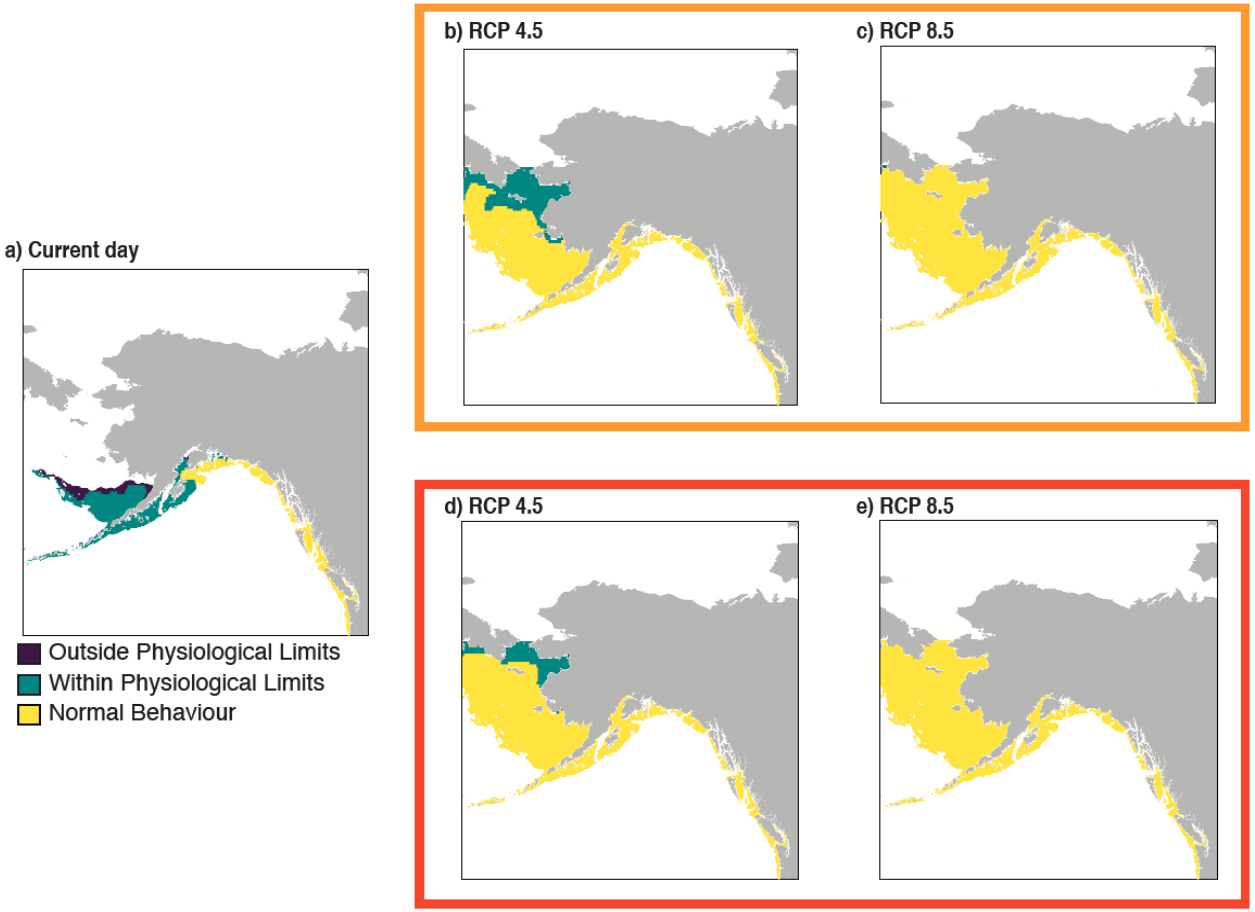

Figure 3. Changes in the projected distribution of marine threespine stickleback (*Gasterosteus aculeatus*) as a result of incorporating thermal traits into models of current day environmental conditions (a) and under IPCC end-of-century projections RCP 4.5 and 8.5, either without trait evolution (b & c; 'no evolution' model, orange box) and with trait evolution (d & e; 'evolution' model, red box)**.**

Table 1. Significant quantitative trait loci (QTL) for critical thermal minimum (CTmin), critical thermal maximum (CTmax), and thermal preference (Preference) traits with the percent of trait variance explained (PVE) for each QTL, the logarithm of odds (LOD) threshold for significance, and the LOD peak observed for each QTL.

QTL Name	Family	Phenotype	Linkage Group	Position	PVE (%)	LOD threshold (5%)	LOD peak
Q1	H1_F2	CTmax	XII	4.56	45.2	2.71	2.87
Q2	H1_F2	Preference	III	50.04	53.3	2.78	3.64
Q3	H2_F2_1	CTmin	III	11.57	28.9	2.55	2.63
Q4	H2_F2_2	CTmin	XXI	55.67	53.7	2.75	3.01
Q5	H2_F2_2	CTmax	XXI	81.36	83.3	5.57	7
Q6	H2_F2_2	Preference	I	108.2	69.3	3.27	4.62
Q7	H2_F2_3	Preference	VII	31.48	87.1	3.61	5.78

Supplementary Figures and Tables

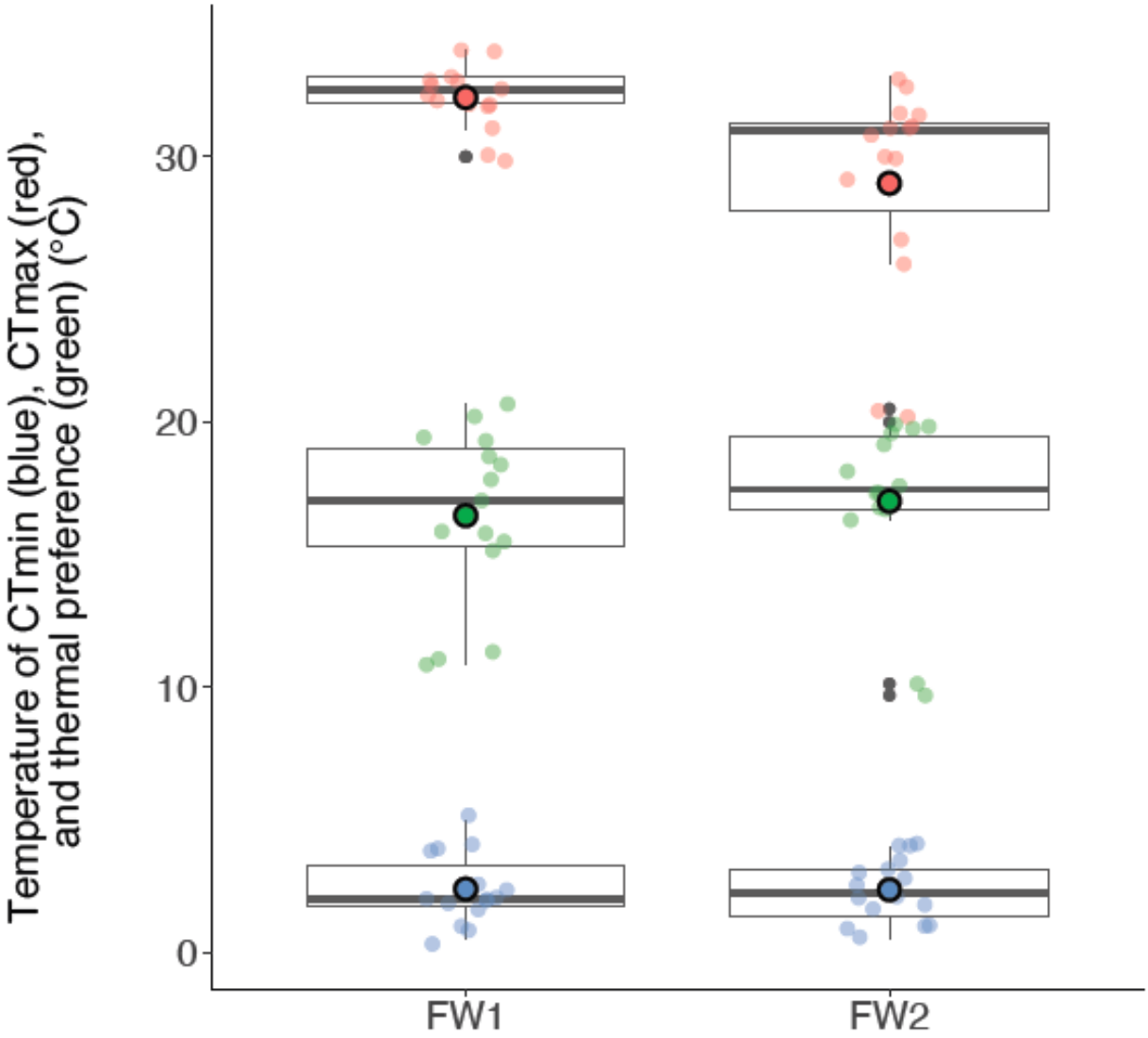

Figure S1. Thermal preference (green), critical thermal minimum (blue) and maximum (red) measurements for adult threespine stickleback (*Gasterosteus aculeatus*) from wild freshwater populations.

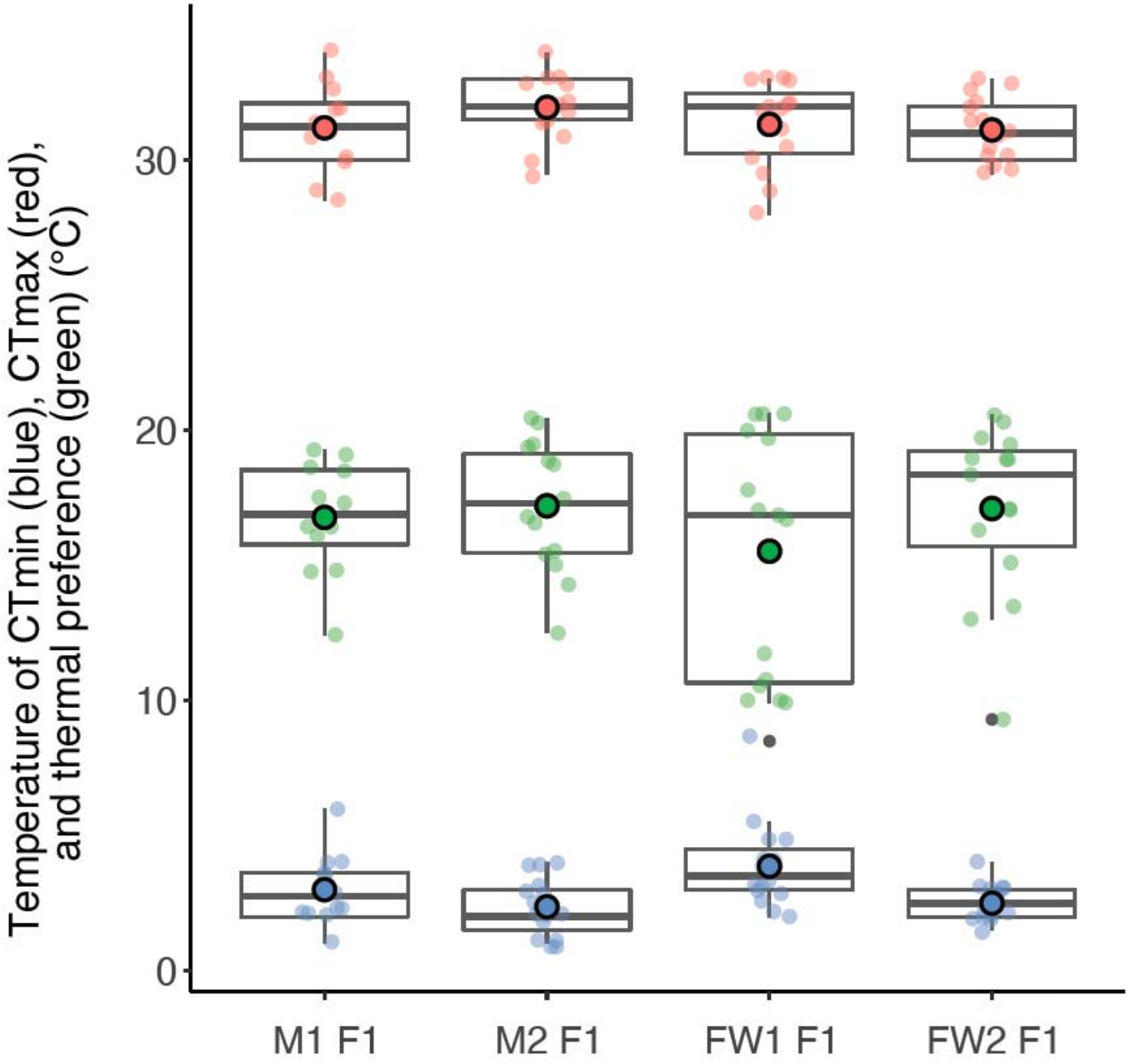

Figure S2. Thermal preference (green), critical thermal minimum (blue) and maximum (red) measurements for adult threespine stickleback (*Gasterosteus aculeatus*) from pure F1 marine (M*F1) and freshwater (FW*F1) families raised in a common garden under a constant thermal environment.

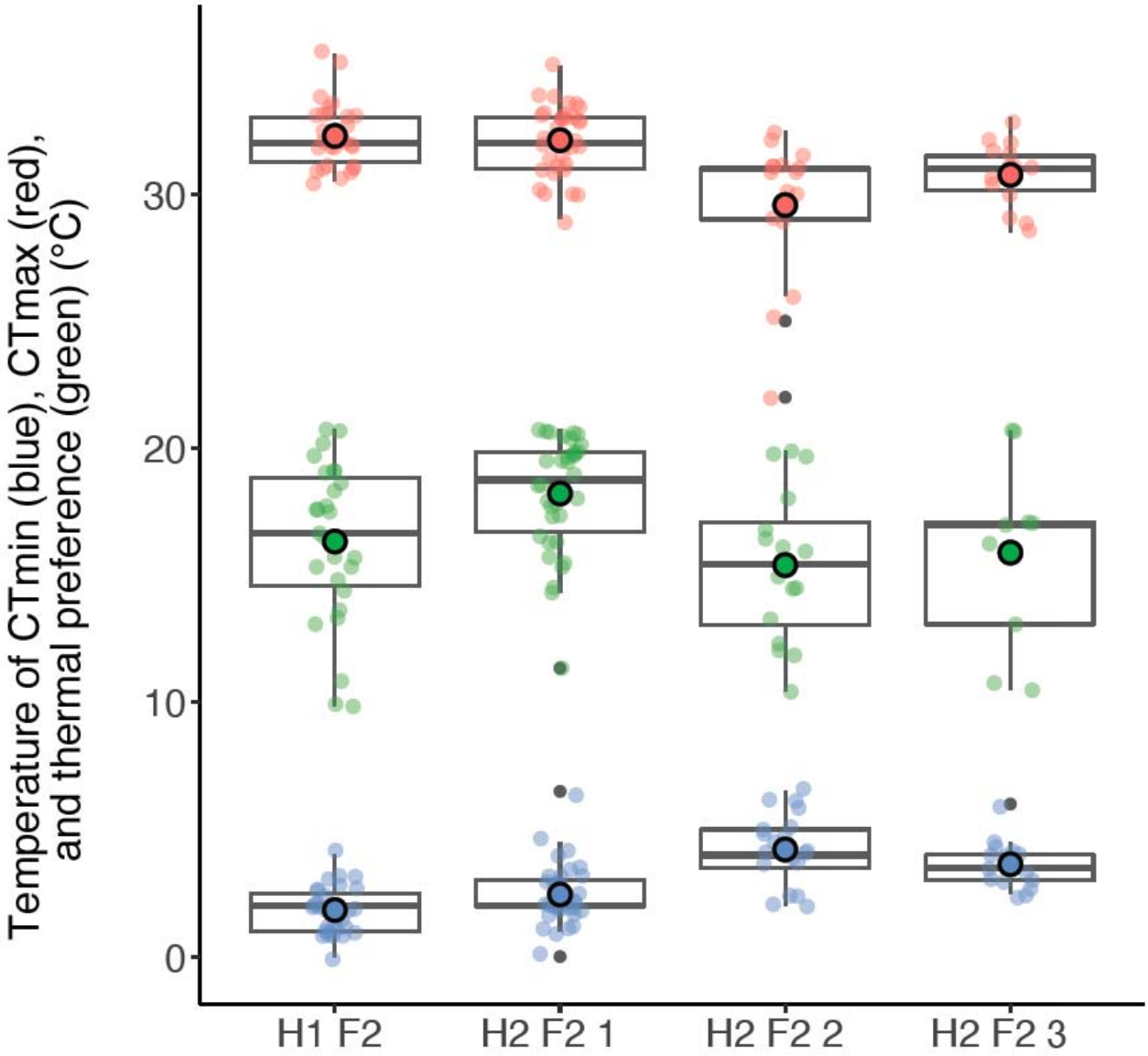

Figure S3. Thermal preference (green), critical thermal minimum (blue) and maximum (red) measurements for adult threespine stickleback (*Gasterosteus aculeatus*) from hybrid marine-freshwater F2 families raised in a common garden under a constant thermal environment.

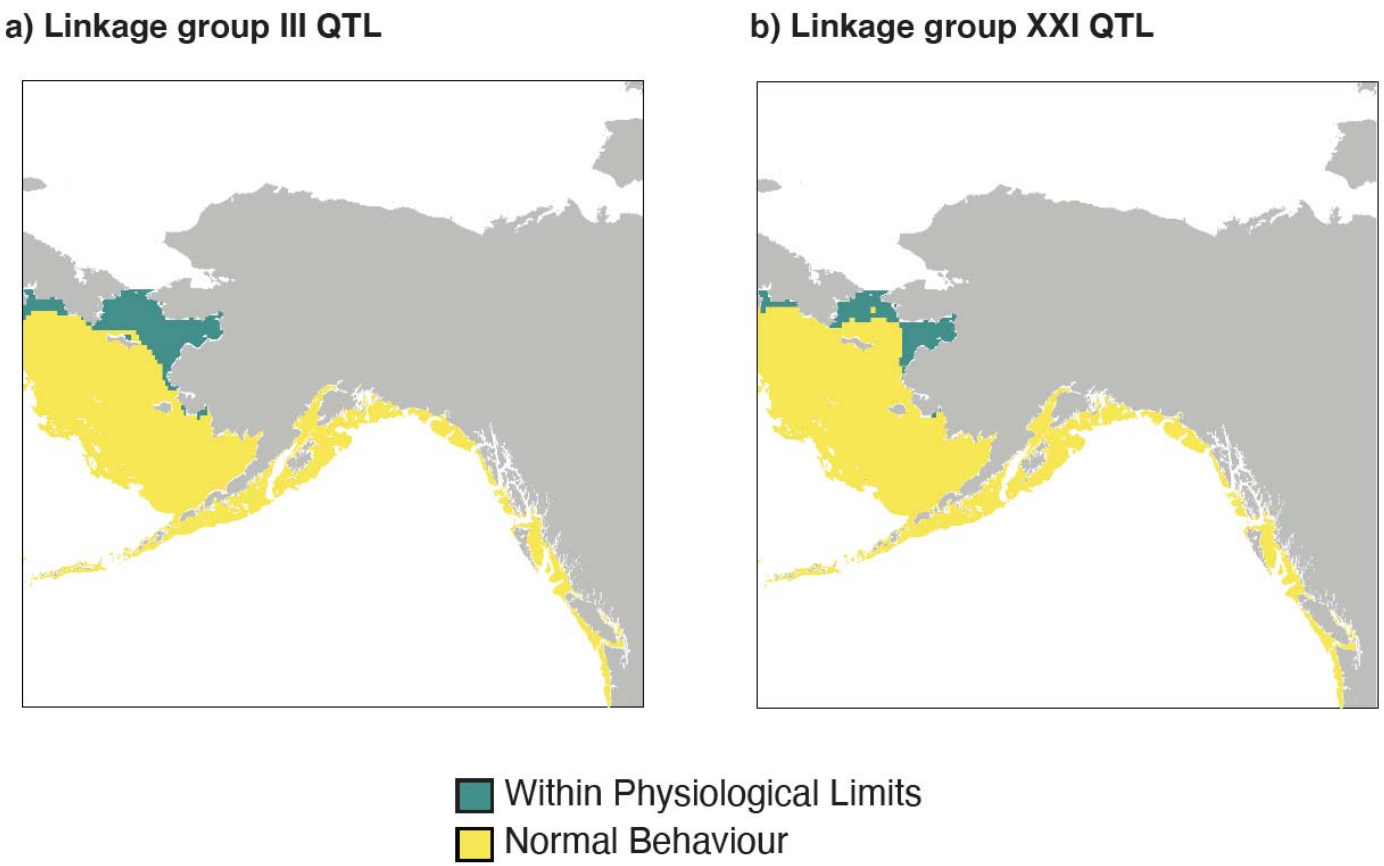

Figure S4. Changes in the distribution of marine threespine stickleback (*Gasterosteus aculeatus*) as a result of incorporating thermal traits under IPCC end-of-century projections RCP 4.5 with trait evolution constrained by the underlying genetic architecture of critical thermal minimum (CTmin) as determined from hybrid F2 mapping families in a) CTmin QTL on linkage group III and b) CTmin QTL on linkage group XXI.

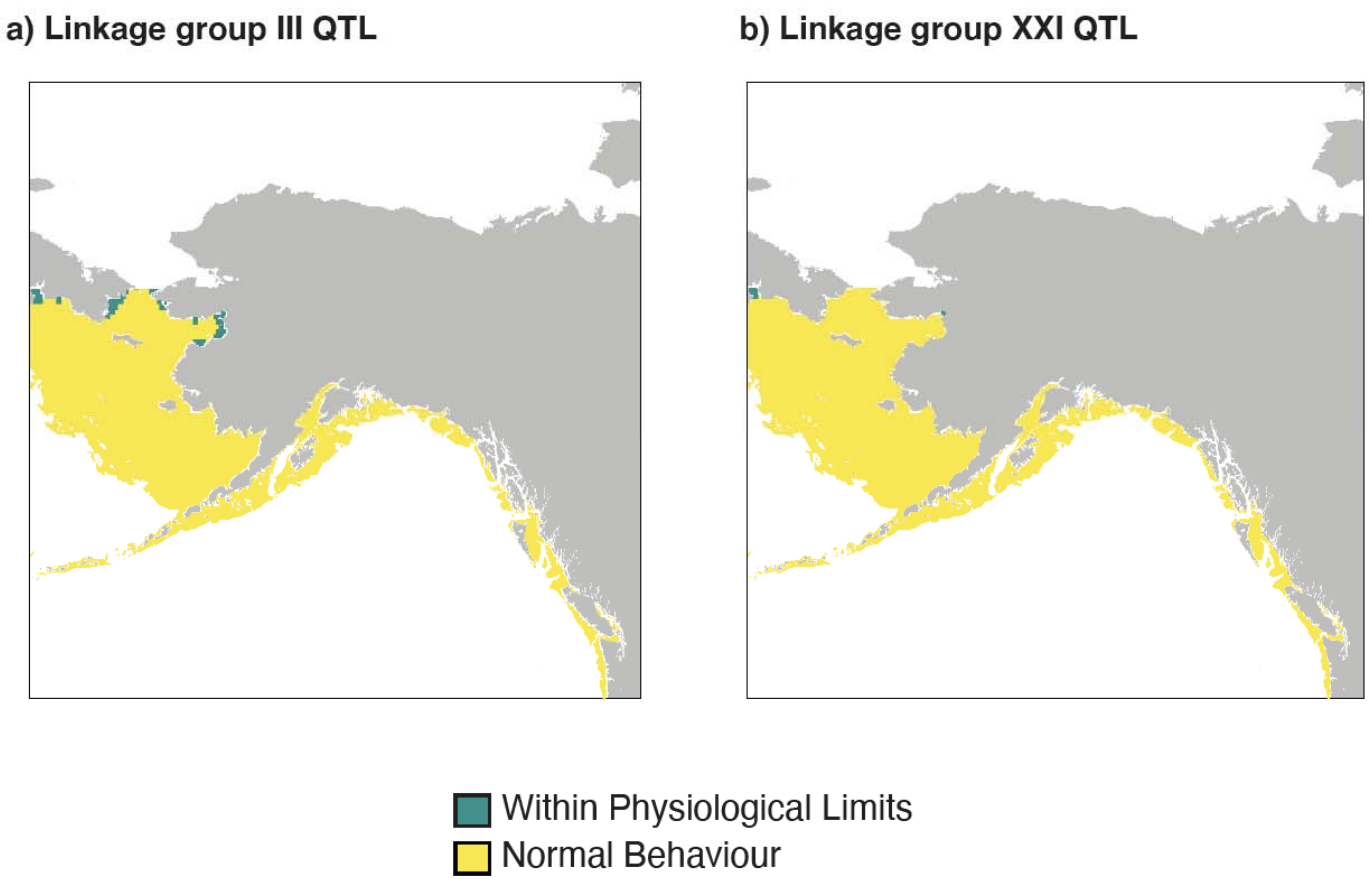

Figure S5. Changes in the distribution of marine threespine stickleback (*Gasterosteus aculeatus*) as a result of incorporating thermal traits under IPCC end-of-century projections RCP 8.5 with trait evolution constrained by the underlying genetic architecture critical thermal maximum (CTmax) as determined from hybrid F2 mapping families in a) CTmin QTL on linkage group III and b) CTmin QTL on linkage group XXI.

Table S1. Summaries of linkage maps constructed for quantitative trait loci (QTL) analyses.

Map	Nmarkers	Length (cM)	Average Maximum Spacing
H1_F2	6571	1678.7	8.98
H2_F2	9930	1995.3	9.36

Table S2. Thermal trait data from *Gasterosteus aculeatus* used to inform the species distribution envelopes (rows) in the varied evolutionary scenarios (columns) projected for end-of-century conditions.

	Current day	No evolution	Evolution	Adjusted PVE - CTmin LG3	Adjusted PVE - CTmin LG21
Normal Behaviour	(5 - 25)	(5 - 25)	(2.5 - 25)	(4.3 - 25)	(3.66 - 25)
Within Physiological Limits	(1.8 - 30.1)	(1.8 - 30.1)	(0 - 30.1)	(1.07 - 30.1)	(0.5 - 30.1)
Outside Physiological Limits	30.1 > x < 1.8	30.1 > x < 1.8	30.1 > x < 0	30.1 > x < 1.07	30.1 > x < 0.5